

Superconductivity and Non-Classical Long-Range Order on a Quantum Computer

LeeAnn M. Sager and David A. Mazziotti*

Department of Chemistry and The James Franck Institute, The University of Chicago, Chicago, IL 60637

(Dated: Submitted June 21, 2021)

An important problem in quantum information is the practical demonstration of non-classical long-range order of quantum computers. One of the best known examples of a quantum system with non-classical long-range order is a superconductor. Here we achieve Cooper pairing of qubits on a quantum computer to represent superconducting or superfluid states. We rigorously confirm the quantum long-range order by measuring the large $O(N)$ eigenvalue of the two-electron reduced density matrix. The demonstration of maximal quantum long-range order is an important step towards more complex modeling of superconductivity and superfluidity as well as other phenomena with significant quantum long-range order on quantum computers.

Introduction: Phenomena like superconductivity and superfluidity arise from a Bose-Einstein-like condensation of fermion pairs into a quantum state with large non-classical long-range order [1–21]. Recently, quantum computers have emerged as potentially powerful calculators of correlated quantum systems [22–30] as high-entanglement states can be programmatically generated at non-exponential cost, which foreshadows the potential emergence of a significant advantage of quantum computers over classical computers for certain classes of problems—a phenomenon known as quantum advantage [31, 32]. Here, we prepare and measure fermion-pair condensates, which can represent superconducting (or superfluid) states, on a transmon-qubit quantum computer.

Pairs of qubits, representing fermions through a Jordan-Wigner mapping, are entangled into Cooper-like bosonic pairs (see Fig. 1) to form superconducting-like states—extreme antisymmetrized geminal power (AGP) wave functions [12, 33–43]. As originally shown by Yang [34, 44] and Coleman [36, 38], such states are extreme in the set of two-electron reduced density matrices (2-RDM), exhibiting the largest possible eigenvalue of the 2-RDM on the order of the number N of electrons $O(N)$ that represents the maximum possible number of Cooper pairs in a common two-electron (geminal) eigenfunction of the 2-RDM. We use tomography on the quantum computer to measure the rxr subblock of the 2-RDM [38, 45, 46] containing the large eigenvalue. Diagonalization of this subblock on a classical computer produces the large eigenvalue and confirms the preparation of the extreme states with maximal non-classical (off-diagonal) long-range order [34, 44]. Even though the extreme AGP functions are expressible as projections of product wave functions [36, 38], they have contributions from an exponentially scaling number of orbital-product configurations (see Fig. 2). Moreover, the measurement of the large eigenvalue of the 2-RDM is applicable to confirming non-classical long-range order in a much richer set of quantum states that cannot be expressed as product states, and, hence, the extreme AGP wave functions in

this work can potentially be modified to generate more complicated, non-product superconducting (superfluid) states for the exploration of more realistic superconducting (superfluid) materials as well as quantum advantage.

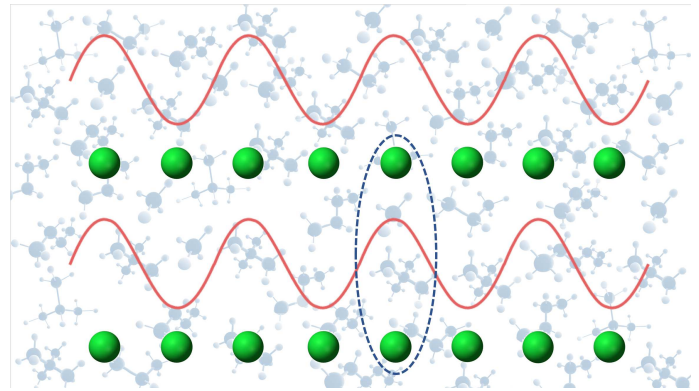


FIG. 1: A schematic demonstrating the interpretation of the Cooper pairing of electrons to create an overall bosonic state in a quantum system.

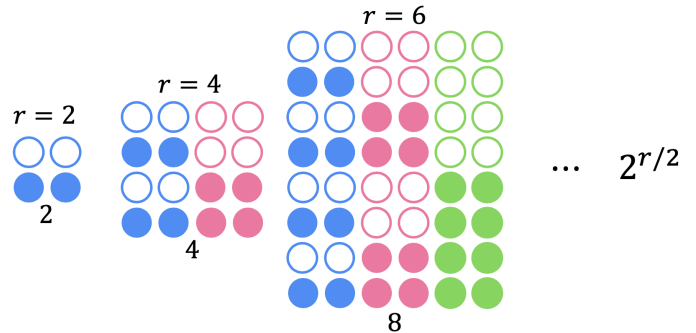


FIG. 2: A schematic demonstrating the possible configurations (i.e., each row) for a given number r of qubits where a filled circle indicates the $|1\rangle$ state which corresponds to an occupied orbital and an unfilled circle represents the $|0\rangle$ state which corresponds to an unoccupied orbital.

* damazz@uchicago.edu

The Superconducting Wavefunction: The superconducting state on the quantum computer is prepared by entangling pairs of qubits into Cooper-like bosonic states. Consider the creation of a state with a Cooper pair of electrons, an extreme geminal [2, 36–38], from the vacuum state

$$|g\rangle = \sum_j e^{i\theta} \hat{a}_j^\dagger \hat{a}_{\bar{j}}^\dagger |\emptyset\rangle \quad (1)$$

where j and \bar{j} are the indices of the paired orbitals ϕ_j and $\phi_{\bar{j}}$, the sum over j is taken with respect to all pairs, and θ is an arbitrary global phase. If we represent each orbital by a qubit with the $|0\rangle$ state representing an un-filled orbital and the $|1\rangle$ state representing a filled orbital, we can use the Jordan-Wigner mapping [47]

$$\hat{a}_j^\dagger = e^{i\pi \sum_{k=1}^{j-1} \sigma_k^+ \sigma_k^-} \sigma_j^+ \quad (2)$$

to map the fermionic operators in Eq. (1) to qubit operators to obtain

$$|g\rangle = \sum_j e^{i\theta} e^{i\pi \sum_{k=1}^{\bar{j}-1} \sigma_k^+ \sigma_k^-} \sigma_j^+ e^{i\pi \sum_{k=1}^{j-1} \sigma_k^+ \sigma_k^-} \sigma_{\bar{j}}^+ |\emptyset\rangle. \quad (3)$$

If the paired orbital indices j and \bar{j} are selected to be consecutive integers in the range $[1, r]$ where r is the total number of orbitals, then the Klein transformations [48] in Eq. (3) simplify to a negative global phase which we can cancel by selecting $\theta = \pi$ to obtain

$$|g\rangle = \sum_j \sigma_j^+ \sigma_{\bar{j}}^+ |\emptyset\rangle. \quad (4)$$

Hence, the extreme geminal of the Cooper pair $|g_{j\bar{j}}\rangle$ of electrons can be represented as two-qubit excitations without approximation. The difference between the fermion and qubit statistics, typically included through an explicit many-qubit Klein transformation, disappears from the pairing of the orbitals to generate an extreme geminal. Moreover, the explicit details of the pairing of the particles is contained within the unspecified orbitals ϕ_j and $\phi_{\bar{j}}$. Consequently, the extreme geminal can physically represent Cooper pairing of electrons in a superconductor or a superfluid in addition to representing even the Cooper-like pairing of bosons [49] or qubits which are paraparticles [50, 51].

The N -electron extreme AGP wave function $|\Psi_{\text{AGP}}^N\rangle$ for even N can be generated from the wedge product of the extreme geminal with itself $N/2$ times [36–38, 52]

$$|\Psi_{\text{AGP}}^N\rangle = |g(12)\rangle \wedge |g(34)\rangle \wedge \dots \wedge |g((N-1)N)\rangle \quad (5)$$

where the wedge \wedge denotes the sum of all products resulting from the antisymmetric permutation of the particles. We can also consider a wave function $|\Psi_{\text{AGP}}\rangle$, also known as a Bardeen-Cooper-Schrieffer (BCS) wave function [1], that is a linear combination of the $|\Psi_{\text{AGP}}^N\rangle$ for all N which is expressible as a product state

$$|\Psi_{\text{AGP}}\rangle = \prod_{j=1}^{r/2} (1 + e^{i\theta} \hat{a}_{2j}^\dagger \hat{a}_{2j-1}^\dagger) |\emptyset\rangle. \quad (6)$$

Using the Jordan-Wigner transformation and simplifying as above, we can generate the AGP state in Eq. (6) with the qubit excitation operators

$$|\Psi_{\text{AGP}}\rangle = \prod_{j=1}^{r/2} (1 + \hat{\sigma}_{2j}^+ \hat{\sigma}_{2j-1}^+) |\emptyset\rangle, \quad (7)$$

which can also be cast as the tensor multiplication of $r/2$ distinct extreme geminals (or the $|\Phi^+\rangle$ Bell states [53])

$$|\Psi_{\text{AGP}}\rangle = \bigotimes_{j=1}^{r/2} \frac{1}{\sqrt{2}} [|00\rangle_{2j,2j-1} + |11\rangle_{2j,2j-1}] \quad (8)$$

where j specifies the pair index and adjacent qubits with qubit indices $2j-1$ and $2j$ are paired by definition.

The above preparation yields an entangled state composed of substates with all possible, paired, even-numbered excitations. See the Supplemental Materials for the gate sequence utilized to obtain this quantum state. On the quantum computer, the extreme AGP state is physically composed of Cooper-like pairs of qubits. Because the phase changes from the fermionic statistics are lost in the pairing—as seen in the above fermionic encoding of the qubits—the extreme state rigorously represents not only entangled pairs of qubits but also Cooper pairs of electrons that are entangled in superconducting or superfluid states. Moreover, the state can represent any physical model for pairing as the precise nature of the pairing (i.e. the pairing of electrons in physical space or in momentum space) is contained in the paired orbitals ϕ_j and $\phi_{\bar{j}}$, which are left unspecified. All pairing states have fundamental entanglement and order properties that are independent of the physical definition of the orbitals. The non-classical long-range order of the extreme AGP state can be assessed from the number of Cooper pairs in the same extreme geminal, which is determinable from the largest eigenvalue of the 2-RDM [34–36].

The Signature of Superconductivity: In order to measure whether the experimentally-prepared quantum state and/or the number-conserving substates projected out from the overall ensemble state demonstrate superconductivity, we conduct quantum tomography (see the Supplemental Materials for details) to probe directly the presence and extent of off-diagonal long-range order, which is a computational signature of superconductivity. To determine the presence and degree of this long-range order for a specified quantum state, it is useful to establish a calculable, characteristic property [12, 33–36, 38–40]. Such a signature of superconductivity is a large eigenvalue in the 2-RDM, which we denote as λ_D [34, 35]. While the entire 2-RDM can be measured by quantum tomography, only the following rxr subblock of the 2-RDM

$${}^2D_{k\bar{k}}^{j\bar{j}} = \langle \Psi_{\text{AGP}} | \hat{a}_j^\dagger \hat{a}_{\bar{j}}^\dagger \hat{a}_{\bar{k}} \hat{a}_k | \Psi_{\text{AGP}} \rangle \quad (9)$$

is required due to the block diagonal structure of the 2-RDM of the AGP wave function. After Jordan-Wigner

transformation to the qubit representation, we can equivalently represent this block of the 2-RDM in terms of the qubit excitation operators as

$${}^2D_{k\bar{k}}^{j\bar{j}} = \langle \Psi_{\text{AGP}} | \hat{\sigma}_j^\dagger \hat{\sigma}_{\bar{j}}^\dagger \hat{\sigma}_{\bar{k}} \hat{\sigma}_k | \Psi_{\text{AGP}} \rangle. \quad (10)$$

For fixed number N of electrons, if the 2-RDM is normalized to $N(N-1)$ as in second quantization, the maximum eigenvalue for even N is bounded from above by N as shown by Yang [34] and Sasaki [35]. Moreover, for a finite rank of r orbitals, this bound can be further tightened [36, 38] to

$$\lambda_D \leq N \left(1 - \frac{N-2}{r} \right). \quad (11)$$

While the thermodynamic limit is not reached until $r \rightarrow \infty$, even for finite r , as long as $N \geq 4$, the 2-RDM exhibits a large eigenvalue that represents the non-classical long-range order associated with Cooper pairing. The 2-RDM from the non-number conserving extreme AGP state $|\Psi_{\text{AGP}}\rangle$ also exhibits a large eigenvalue, representing an average of the Cooper pairs in each of the fixed- N extreme AGP states. The number-conserving blocks of the 2-RDM with even particle numbers—i.e., 2-RDMs of zero, two, four, ..., $r-2$, and r particles for an r -qubit system—can be determined from the non-number conserving state via post-measurement analysis (see the Supplemental Materials). Analysis on the presence and extent of superconductivity (measured via λ_D) of both the overall entangled state ($|\Psi\rangle$) and the number-conserving substates is conducted for various numbers r of total qubits in the following sections.

Results: The extreme non-number conserving AGP state is prepared for both simulation and an experimental quantum device for all even-numbered qubit systems from $r = 0$ to $r = 14$. Post-measurement computation of the quantum signature of superconductivity (λ_D) is then employed to probe the presence and extent of superconductivity for these overall states. As can be seen in Figure 3, the signature of superconductivity increases as the number r of qubits comprising the system is increased, and—for simulation—superconductivity is observed (i.e., $\lambda_D > 1$) for all prepared states with $r \geq 8$. While the experimental results deviate from simulation due to the noisy nature of near-term quantum devices [54] (see Supplemental Materials for device specifications and errors), experimental systems with $r = 12$ and $r = 14$ qubits did demonstrate superconductivity. Further, the trend of the extent of superconductivity increasing as the number of qubits comprising the system increases holds for the experimental results, which is promising for future benchmarking of quantum computers through the preparation of extreme superconducting states with larger number of qubits as well as efforts to probe more macroscopically-scaled superconducting materials on quantum devices.

The non-number conserving extreme AGP state has contributions to the large eigenvalue from multiple number-conserving substates, and hence, the magnitude

of this eigenvalue is less than that of the substates around the center of the number distribution $N \approx r/2$. Additionally, real-world superconducting materials should conserve particle number. It is hence beneficial to probe the number-conserving substates that comprise the overall entangled state in order to both isolate the superconducting behavior of the number-conserving substates and to more-closely model real-world superconductivity.

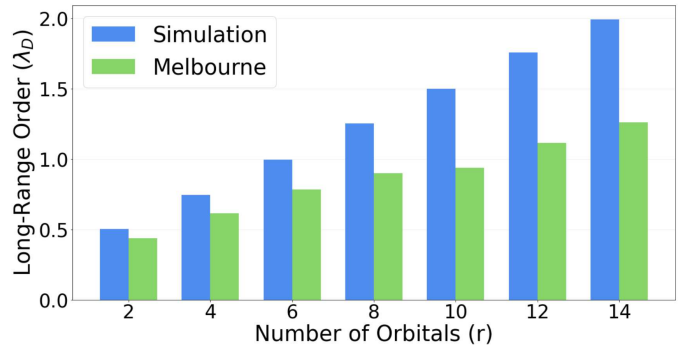


FIG. 3: The λ_D values for the overall ensemble state preparation for simulation and experimental melbourne results.

By projecting out a specific number of particles from the results obtained for overall entangled state (see the Supplemental Materials), we can probe the behavior and properties of the number-conserving substates. Specifically, as is shown in Fig. 4, the extent of superconductivity (λ_D) for each number-conserving state can be isolated from the overall r -qubit preparation described in Eq. (8). As can be seen from the simulation results, all number-conserving substates with $2 < N < r$ demonstrate superconductivity ($\lambda_D > 1$) where $N = 2$ fails to demonstrate condensation behavior as the maximum signature of condensation is $N/2$ for even N -particle systems [34, 35] and where $N = r$ fails to demonstrate condensation behavior as this substate $|1\rangle^{\otimes r}$ is not entangled. Further, the signature of condensation seems to follow a bell curve centered around $(r+2)/2$ such that maximum superconductivity is observed at half filling for $N = (r+2)/2$ if $(r+2)/2$ is even and for both $N = (r+2)/2 - 1$ and $(r+2)/2 + 1$ if $(r+2)/2$ is odd. Again, the extent of superconductivity is lesser for the experimental results for all particle-conserving states due to experimental error; however, the qualitative trends described for simulation hold in general although the bell curve does demonstrate a slight negative (right-modal) skew, implying that the quantum computer does not exactly treat the particle and hole statistics symmetrically. Importantly, superconductivity is clearly observed for $r = 14$ experimental results for particle numbers $N \geq 6$. Note that although only results for the largest-qubit preparation $r = 14$ are shown, all data is included in the Supplemental Materials; the trends in the $r = 14$ data hold for the lower-qubit results, and additionally, the $r = 14$ qubit data demon-

strates the largest signature of superconductivity as the largest eigenvalue λ_D value for a fixed N increases as the number r of qubits is increased.

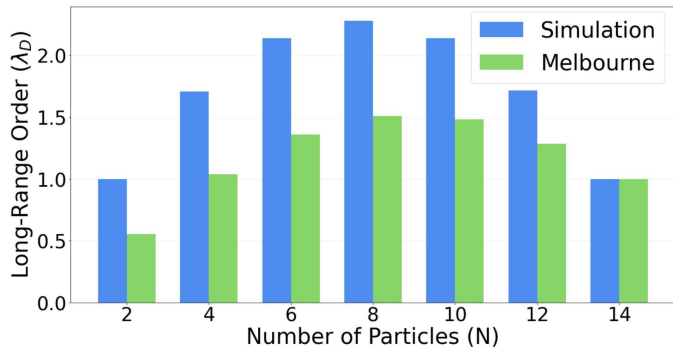


FIG. 4: The λ_D values for the number-conserving sub-states of rank $r = 14$ for simulation and experimental melbourne results.

Conclusions: Here we prepare superconducting states from the Cooper pairing of qubits on a transmon quantum computer—where each qubit is composed of a microwave phonon in an anharmonic well potential. Using the Jordan-Wigner mapping between fermions and qubits, we rigorously show that the prepared states are equally valid representations of condensations of Cooper pairs of fermions, bosons, or qubits. Hence, such Cooper-pair-based condensations and their associated non-classical long-range order are independent of the particle statistics. Moreover, the prepared states are also independent of the physical details of the paired orbitals, and consequently, are representative of superconducting, superfluid, or other pairing states. The studied states are known as extreme AGPs because they exhibit the maximum degree of non-classical (off-diagonal) long-range order as determined by the number of Cooper pairs in the same geminal state, which is equal to the largest eigenvalue of the 2-RDM [2, 34–36, 38, 41, 44]. We measure an rxr subblock of the 2-RDM [38, 45, 46] on the quantum computer and compute its largest eigenvalue on a classical computer. We observe large eigenvalues both for the non-particle conserving extreme AGP state and the particle-conserving extreme AGP substates. The large eigenvalues confirm the preparation of these extreme AGP states, which are the only states to exhibit the largest possible eigenvalues [38], as well as the generation of maximum non-classical long-range order.

The upper bound on the largest eigenvalue of the 2-RDM, $\lambda_D = N$, is technically only reached in the thermodynamic limit of $r \rightarrow \infty$. However, as seen in Eq. (11), the large eigenvalue is rapidly approached with increasing r as the fraction of Cooper pairs that are removed from the condensate due to finite size effects scales as $1/r$.

Consequently, the quantum long-range order as well as its associated entanglement begin to appear for the range of r ($r \leq 14$) explored in the present study. On both a quantum simulator and an IBM quantum computer, we observe that the large eigenvalue follows the expected bell curve with respect to r . The known value for the maximum eigenvalue of the extreme AGP state provides a clear metric for not only confirming the presence of the extreme state and its long-range order but also benchmarking the fidelity with respect to noise of both current and future quantum computers.

An aspirational goal of quantum computing is to achieve a quantum advantage over traditional classical computing for the solution of a significant problem. One such area of chemistry and physics, which traces back to the original proposal of Feynman [55], is the simulation of molecules on quantum computers. The construction of the wave function on a classical computer scales exponentially in the number of orbital-based configurations. In principle, the quantum computer offers the possibility of preparing and measuring quantum states with non-exponential scaling. This possibility depends on the complexity of the necessary state preparation. In the present case, the extreme AGP wave function is a product state composed of a product of extreme geminals (or Bell states). Consequently, the maximum degree of non-classical long-range order, at least as measured by the largest eigenvalue of the 2-RDM, can be achieved with polynomial cost on both classical and quantum computers. The extreme AGP states, nonetheless, provide an intriguing reference for the exploration of more complicated superconducting states with large eigenvalues that cannot be easily expressed as product-state wave functions. From this perspective, the present work of preparing and measuring superconducting states from Cooper pairs of qubits on a quantum computer provides an initial step towards preparing more complicated condensates of Cooper pairs—with potential future applications to the study of both superconducting materials and quantum simulation.

Supplemental Material: The Supplemental Material (SM) contains the quantum algorithm for state preparation, a description of noise on near-term quantum devices, device data on the quantum computers, additional tomography data, tomography protocol for the two-particle reduced density matrix, additional large eigenvalue data, and experimental quantum device specifications.

ACKNOWLEDGMENTS

D.A.M. gratefully acknowledges the Department of Energy, Office of Basic Energy Sciences, Grant DE-SC0019215 and the U.S. National Science Foundation Grants No. CHE-2035876, No. DMR-2037783, and No. CHE-1565638.

- [1] J. Bardeen, L. N. Cooper, and J. R. Schrieffer, Theory of superconductivity, *Phys. Rev.* **108**, 1175 (1957).
- [2] J. M. Blatt, Electron pairs in the theory of superconductivity, *Prog. Theor. Phys.* **23**, 447 (1960).
- [3] P. W. Anderson, Twenty-five years of high-temperature superconductivity – a personal review, *J. Phys.: Conf. Ser.* **449**, 012001 (2013).
- [4] A. P. Drozdov, P. P. Kong, V. S. Minkov, S. P. Besedin, M. A. Kuzovnikov, S. Mozaffari, L. Balicas, F. F. Balakirev, D. E. Graf, V. B. Prakapenka, E. Greenberg, D. A. Knyazev, M. Tkacz, and M. I. Eremets, Superconductivity at 250 K in lanthanum hydride under high pressures, *Nature* **569**, 528 (2019).
- [5] V. L. Ginzburg, High-temperature superconductivity (history and general review), *Sov. Phys. Usp.* **34**, 283 (1991).
- [6] A. Glatz, I. A. Sadovskyy, U. Welp, W.-K. Kwok, and G. W. Crabtree, The quest for high critical current in applied high-temperature superconductors, *J. Supercond. Nov. Magn.* **33**, 127–141 (2020).
- [7] Y. Cao, V. Fatemi, S. Fang, K. Watanabe, T. Taniguchi, E. Kaxiras, and P. Jarillo-Herrero, Unconventional superconductivity in magic-angle graphene superlattices, *Nature* **556**, 43–50 (2018).
- [8] Y. Cao, D. Rodan-Legrain, O. Rubies-Bigorda, J. M. Park, K. Watanabe, T. Taniguchi, and P. Jarillo-Herrero, Tunable correlated states and spin-polarized phases in twisted bilayer–bilayer graphene, *Nature* **583**, 215–220 (2020).
- [9] A. Uri, S. Grover, Y. Cao, J. Crosse, K. Bagani, D. Rodan-Legrain, Y. Myasoedov, K. Watanabe, T. Taniguchi, P. Moon, and et al., Mapping the twist-angle disorder and Landau levels in magic-angle graphene, *Nature* **581**, 47–52 (2020).
- [10] E. Tutuc, M. Shayegan, and D. A. Huse, Counterflow measurements in strongly correlated GaAs hole bilayers: evidence for electron-hole pairing, *Phys. Rev. Lett.* **93**, 36802 (2004).
- [11] D. V. Fil and S. I. Shevchenko, Electron-hole superconductivity (review), *Low Temp. Phys.* **44**, 867 (2018).
- [12] S. Safaei and D. A. Mazziotti, Quantum signature of exciton condensation, *Phys. Rev. B* **98**, 045122 (2018).
- [13] A. Kogar, M. S. Rak, S. Vig, A. A. Husain, F. Flicker, Y. I. Joe, L. Venema, G. J. MacDougall, T. C. Chiang, E. Fradkin, J. van Wezel, and P. Abbamonte, Signatures of exciton condensation in a transition metal dichalcogenide, *Science* **358**, 1314 (2017).
- [14] X. Liu, K. Watanabe, T. Taniguchi, B. I. Halperin, and P. Kim, Quantum Hall drag of exciton condensate in graphene, *Nat. Phys.* **13**, 746 (2017).
- [15] F. London, *Superfluids: Macroscopic theory of superconductivity*, Structure of Matter Series (Wiley, 1950).
- [16] R. P. Feynman, *Chapter II Application of Quantum Mechanics*, edited by C. Gorter, Progress in Low Temperature Physics, Vol. 1 (Elsevier, 1955) pp. 17–53.
- [17] A. J. Leggett, Superfluidity, *Rev. Mod. Phys.* **71**, S318 (1999).
- [18] C. Gorter, *Progress in Low Temperature Physics* (Elsevier Science, 2011).
- [19] Y. Guo, R. Dubessy, M. de Herve, A. Kumar, T. Badr, A. Perrin, L. Longchambon, and H. Perrin, Supersonic rotation of a superfluid: A long-lived dynamical ring, *Phys. Rev. Lett.* **124**, 025301 (2020).
- [20] Y. Hao, S. Pang, X. Zhang, and L. Jiang, Quantum-confined superfluid reactions, *Chem. Sci.* **11**, 10035 (2020).
- [21] G. Del Pace, W. J. Kwon, M. Zaccanti, G. Roati, and F. Scazza, Tunneling transport of unitary fermions across the superfluid transition, *Phys. Rev. Lett.* **126**, 055301 (2021).
- [22] F. Verstraete, J. I. Cirac, and J. I. Latorre, Quantum circuits for strongly correlated quantum systems, *Phys. Rev. A* **79** (2009).
- [23] A. Smith, M. S. Kim, F. Pollmann, and J. Knolle, Simulating quantum many-body dynamics on a current digital quantum computer, *npj Quantum Inf.* **5** (2019).
- [24] G. J. Mooney, C. D. Hill, and L. C. L. Hollenberg, Entanglement in a 20-qubit superconducting quantum computer, *Sci. Rep.* **9** (2019).
- [25] R. Ma, B. Saxberg, C. Owens, N. Leung, Y. Lu, J. Simon, and D. I. Schuster, A dissipatively stabilized Mott insulator of photons, *Nature* **566**, 51–57 (2019).
- [26] H.-L. Huang, D. Wu, D. Fan, and X. Zhu, Superconducting quantum computing: a review, *Sci. China Inf. Sci.* **63** (2020).
- [27] S. McArdle, S. Endo, A. Aspuru-Guzik, S. C. Benjamin, and X. Yuan, Quantum computational chemistry, *Rev. Mod. Phys.* **92** (2020).
- [28] K. Head-Marsden, J. Flick, C. J. Ciccarino, and P. Narang, Quantum information and algorithms for correlated quantum matter, *Chem. Rev.* **10.1021/acs.chemrev.0c00620** (2021).
- [29] S. E. Smart and D. A. Mazziotti, Quantum-classical hybrid algorithm using an error-mitigating n - representability condition to compute the mott metal-insulator transition, *Phys. Rev. A* **100**, 10.1103/physreva.100.022517 (2019).
- [30] L. M. Sager, S. E. Smart, and D. A. Mazziotti, Preparation of an exciton condensate of photons on a 53-qubit quantum computer, *Phys. Rev. Research* **2**, 043205 (2020).
- [31] F. Arute, K. Arya, R. Babbush, D. Bacon, J. C. Bardin, R. Barends, R. Biswas, S. Boixo, F. G. S. L. Brandao, D. A. Buell, and et al., Quantum supremacy using a programmable superconducting processor, *Nature* **574**, 505–510 (2019).
- [32] V. E. Elfving, B. W. Broer, M. Webber, J. Gavartin, M. D. Halls, K. P. Lorton, and A. D. Bochevarov, How will quantum computers provide an industrially relevant computational advantage in quantum chemistry?, *arXiv* , 1–20 (2020).
- [33] O. Penrose and L. Onsager, Bose-Einstein condensation and liquid helium, *Phys. Rev.* **104**, 576 (1956).
- [34] L. Onsager, Concept of off-diagonal long-range order and the quantum phases of liquid He and of superconductors, *Rev. Mod. Phys.* **34**, 694 (1962).
- [35] F. Sasaki, Eigenvalues of fermion density matrices, *Phys. Rev.* **138**, B1338 (1965).
- [36] A. J. Coleman, Structure of fermion density matrices, *Rev. Mod. Phys.* **35**, 668 (1963).
- [37] A. J. Coleman, Electron pairs in the quasichemical-equilibrium and Bardeen-Cooper-Schrieffer theories,

- Phys. Rev. Lett.* **13**, 406 (1964).
- [38] A. J. Coleman, Structure of fermion density matrices. II. Antisymmetrized Geminal Powers, *J. Math. Phys.* **6**, 1425 (1963).
- [39] L. M. Sager, S. Safaei, and D. A. Mazziotti, Potential coexistence of exciton and fermion-pair condensations, *Phys. Rev. B* **101**, 081107 (2020).
- [40] A. Raeber and D. A. Mazziotti, Large eigenvalue of the cumulant part of the two-electron reduced density matrix as a measure of off-diagonal long-range order, *Phys. Rev. A* **92**, 052502 (2015).
- [41] J. M. Blatt, *Theory of superconductivity* (Academic Press Inc., 1964).
- [42] F. Bloch, Off-diagonal long-range order and persistent currents in a hollow cylinder, *Phys. Rev.* **137** (1965).
- [43] A. Khamoshi, F. A. Evangelista, and G. E. Scuseria, Correlating AGP on a quantum computer, *Quantum Sci. Technol.* **6**, 014004 (2021).
- [44] A. J. Coleman, The structure of fermion density matrices. III. Long-range order, *J. Low. Temp. Phys.* **74**, 1–17 (1989).
- [45] K. Head-Marsden and D. A. Mazziotti, Pair 2-electron reduced density matrix theory using localized orbitals, *J. Chem. Phys.* **147**, 084101 (2017).
- [46] W. Poelmans, M. Van Raemdonck, B. Verstichel, S. De Baerdemacker, A. Torre, L. Lain, G. E. Massaccesi, D. R. Alcoba, P. Bultinck, and D. Van Neck, Variational optimization of the second-order density matrix corresponding to a seniority-zero configuration interaction wave function, *J. Chem. Theory Comput.* **11**, 4064 (2015).
- [47] P. Jordan and E. Wigner, Über das paulische Äquivalenzverbot, *Eur. Phys. J. A* **47**, 631–651 (1928).
- [48] O. Klein, Quelques remarques sur le traitement approximatif du problème des électrons dans un réseau cristallin par la mécanique quantique, *J. Phys. Radium* **9**, 1 (1938).
- [49] T. Keilmann and J. J. García-Ripoll, Dynamical creation of bosonic Cooper-like pairs, *Phys. Rev. Lett.* **100**, 110406 (2008).
- [50] L.-A. Wu and D. A. Lidar, Qubits as parafermions, *J. Math. Phys.* **43**, 4506 (2002).
- [51] D. A. Mazziotti and A. R. Mazziotti, Quantum simulation of molecules without fermionic encoding of the wave function, *arXiv* (2021).
- [52] K. Naftchi-Ardebili, N. W. Hau, and D. A. Mazziotti, Rank restriction for the variational calculation of two-electron reduced density matrices of many-electron atoms and molecules, *Phys. Rev. A* **84**, 052506 (2011).
- [53] M. Nielsen and I. Chuang, *Quantum Computation and Quantum Information: 10th Anniversary Edition* (Cambridge University Press, 2010).
- [54] J. Preskill, Quantum computing in the NISQ era and beyond, *Quantum* **2**, 79 (2018).
- [55] R. P. Feynman, Simulating physics with computers, *Int. J. Theor. Phys.* **21**, 467–488 (1982).